

for calling attention to the misprint mentioned in Ref. 2.

APPENDIX

Using the same notation as in Ref. 2, the value of the various parameters⁹⁻¹¹ used in the computations were $C_C=0$, $A_C=0.64\times 10^{-12}$ cm, $C_d=-0.41\times 10^{-12}$

⁹ N. K. Pope, Can. J. Phys. **30**, 597 (1952).

¹⁰ G. E. Bacon, *Neutron Diffraction* (Oxford University Press, London, 1955) p. 125.

¹¹ T. Y. Wu, *Vibrational Spectra and Structure of Polyatomic Molecules* (Edwards Brothers, Inc., Ann Arbor, Michigan, 1946).

cm, $A_d=0.65\times 10^{-12}$ cm, $b=1.093\times 10^{-8}$ cm, $I=10.66\times 10^{-40}$ g cm², $\gamma_{dd}=4.02\times 10^{-19}$ cm², $\gamma_{CC}=3.57\times 10^{-20}$ cm², and $M=53.51\times 10^{-24}$ g.

The values for γ_{dd} and γ_{CC} were obtained by using the results of Ref. 9. The bound coherent scattering length A_d and the bound incoherent scattering length C_d were obtained by using the scattering lengths of Ref. 10 in their definitions.¹ It is perhaps worth mentioning that with an incident-neutron energy of 0.10 eV, there will be no vibrational states excited since the lowest vibrational state¹¹ of CD₄ is about 0.12 eV.

Excitation of Ion-Acoustic Waves

R. W. GOULD*

Institut für Plasmaphysik, Garching bei München, Germany

(Received 11 May 1964)

The excitation of ion-acoustic waves by a pair of idealized grids in a collisionless plasma is examined. It is shown that in a limited region, neither too close nor too far from the source, the disturbance closely approximates an exponentially damped (spatially) ion-acoustic wave. Far from the source a weak electron "wave" with less damping and larger wavelength dominates; near the source the potential varies as $1/z$.

I. INTRODUCTION

THE velocity and damping of ion-acoustic waves in cesium and potassium plasmas have been measured by Wong, D'Angelo, and Motley.¹ Since this is the only experiment to date which seems to confirm the existence of Landau damping² it is important to examine the interpretation of the experimental results carefully. In this note we examine the excitation of ion-acoustic waves by a source in a collisionless unbounded plasma. We show that, *in general*, ion waves cannot be interpreted by simply examining a single root of the dispersion relation. However, we find that in a region of a few wavelengths in extent, neither too close to the source nor too far, the disturbance from an idealized sinusoidally driven pair of grids has a wavelike character with approximately exponential damping.

In obtaining this result we make use of the Fourier transform (or superposition) method together with a frequency- and wave-number-dependent complex dielectric constant.

II. DISPERSION EQUATION FOR ION-ACOUSTIC WAVES

The complex dielectric constant for small amplitude longitudinal waves in a hot collisionless plasma may be

* On leave from the California Institute of Technology, Pasadena, California.

¹ A. Y. Wong, N. D'Angelo, and R. W. Motley, Phys. Rev. Letters **9**, 415 (1962); Phys. Rev. **133**, A436 (1964).

² L. D. Landau, J. Phys. (USSR) **10**, 25 (1946).

written³

$$K(\omega, k) = \frac{1}{k^2} \int \frac{\mathbf{k} \cdot \nabla_v (\omega_{pi}^2 F_0 + \omega_{pe}^2 f_0)}{(\omega - \mathbf{k} \cdot \mathbf{v})} d^3v, \quad (1)$$

where a space and time dependence of $e^{i(\mathbf{k} \cdot \mathbf{r} - \omega t)}$ is assumed. F_0 and f_0 are the normalized ion and electron velocity distribution functions, respectively, and $\omega_{pi} = (Ne^2/\epsilon_0 M_i)^{1/2}$ and $\omega_{pe} = (Ne^2/\epsilon_0 M_e)^{1/2}$ are the ion and electron plasma frequencies, respectively. The velocity integrals are to be evaluated assuming ω to have a *small positive* imaginary part (corresponding to having "turned on" the sources in the past) and k to be real (Fourier transform in space). It is furthermore convenient to regard the dielectric constant as functions of the *complex* variables ω and k in which case analytic continuation, as discussed by Landau,² is implied.

Upon introducing the Maxwell velocity distribution functions

$$F_0 = (\pi^{1/2} v_i)^{-3} \exp(-v^2/v_i^2)$$

and

$$f_0 = (\pi^{1/2} v_e)^{-3} \exp(-v^2/v_e^2),$$

with $v_i = (2\kappa T_i/M_i)^{1/2}$ and $v_e = (2\kappa T_e/M_e)^{1/2}$, the ion and electron thermal speeds, respectively, one obtains

$$K(\omega, k) = 1 - \frac{\omega_{pi}^2}{k^2 v_i^2} Z' \left(\frac{\omega}{k v_i} \right) - \frac{\omega_{pe}^2}{k^2 v_e^2} Z' \left(\frac{\omega}{k v_e} \right), \quad (2)$$

³ B. D. Fried and R. W. Gould, Phys. Fluids **4**, 139 (1961).

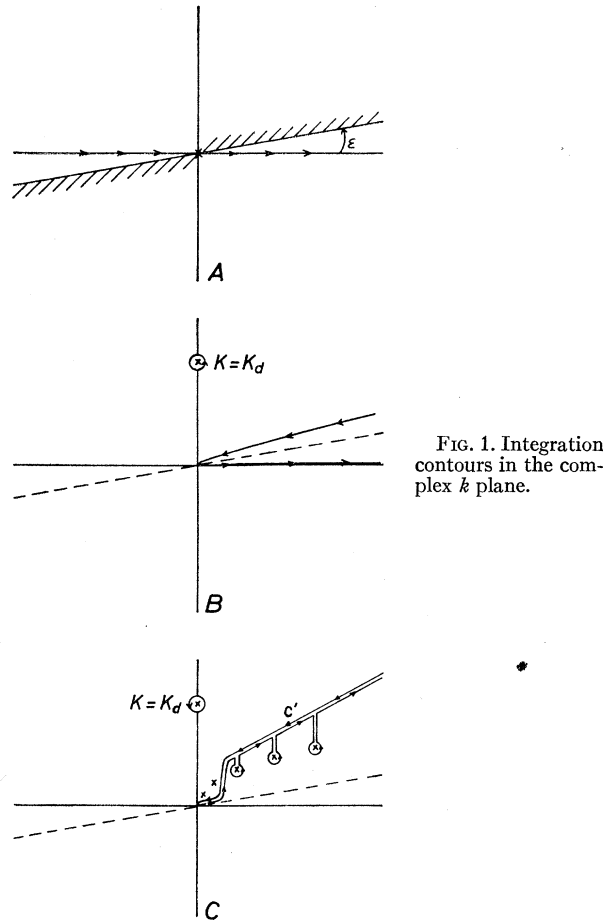


FIG. 1. Integration contours in the complex k plane.

where $Z'(\zeta) = dZ(\zeta)/d\zeta$, and

$$Z(\zeta) = \frac{1}{\sqrt{\pi}} \int_{-\infty}^{\infty} \frac{e^{-x^2}}{x - \zeta} dx, \quad \text{Im}\zeta > 0 \quad (3)$$

is the plasma dispersion function.⁴

The characteristic frequencies of longitudinal ion oscillations are given by the zeros of the dielectric constant. For long wavelengths $\omega_{pi}^2/k^2v_i^2$ and $\omega_{pe}^2/k^2v_e^2$ are much greater than unity and $\omega/kv_e \ll 1$. Thus, the dielectric constant may be written approximately

$$K(\omega, k) = \frac{\omega_{pi}^2}{k^2v_i^2} \left[2 \frac{T_i}{T_e} - Z' \left(\frac{\omega}{kv_i} \right) \right]. \quad (4)$$

The characteristic frequencies for long-wavelength oscillations are therefore given approximately by the solutions of the equation $Z'(\omega/kv_i) = 2T_i/T_e$. The first few solutions for the case $T_e = T_i$, obtained with the aid of Ref. 4, are shown in Table I. The first entry gives the least damped solution of the initial value problem²

TABLE I. Solutions of the equation $Z'(\omega_0/kv_i) = 2$.

j	$(\omega_0/kv_i)_j$	$\eta_j = (kv/\omega_0)_j$
1	1.45 - 0.60 <i>i</i>	0.59 + 0.243 <i>i</i>
2	2.36 - 1.79 <i>i</i>	0.259 + 0.204 <i>i</i>
3	2.98 - 2.49 <i>i</i>	0.198 + 0.164 <i>i</i>
4	3.37 - 3.04 <i>i</i>	0.164 + 0.147 <i>i</i>
5	3.9 - 3.5 <i>i</i>	0.14 + 0.13 <i>i</i>

(k real) and is the one which one would normally expect to dominate after a long time.

However, in a wave experiment the frequency ω is real (and the source localized) and one expects a *spatial* Landau damping (complex k) instead of a temporal damping. It is tempting, therefore, to examine the zeros of Eqs. (2) or (4) to obtain the velocity and damping (or real and imaginary parts of k) of the characteristic waves. Indeed, in the interpretation of their ion-wave experiments, Wong *et al.*¹ used the first entry in Table I. The difficulty with this procedure is that the first entry in Table I does not represent the solution with *least spatial damping* but instead the one with the *greatest spatial damping*. Furthermore, there are infinitely many solutions of Eq. (4) with less damping, with the limit point $k = 0$. There is also a branch cut integral to be considered as is shown in the next section. Clearly an interpretation in terms of a least damped wave is questionable in the case of spatial damping.

III. EXCITATION OF ION-ACOUSTIC WAVES BY IDEALIZED GRIDS

For sake of definiteness we consider the disturbance induced in the plasma by a pair of closely spaced idealized grids, capable of introducing an "external" oscillating charge density $\sigma_0 e^{-i\omega t} [\delta(x - \frac{1}{2}x_0) - \delta(x + \frac{1}{2}x_0)]$ into the plasma without intercepting particles.⁵ We shall henceforth suppress the factor $e^{-i\omega t}$. The spatial Fourier transform (in one dimension) of the external charge is

$$\rho(k) = -2i\sigma_0 \sin(\frac{1}{2}kx_0) \approx -ik\sigma_0 x_0 \quad kx_0 \ll 1. \quad (5)$$

We shall, for convenience, consider the dipole limit $x_0 \rightarrow 0$, $\sigma_0 x_0 \rightarrow \text{constant}$. The plasma potential may be written

$$\phi(k) = \frac{\rho(k)}{k^2 \epsilon_0 K(\omega, k)} = -i \frac{\sigma_0 x_0}{\epsilon_0} \frac{1}{kK(\omega, k)} \quad (6)$$

where $K(\omega, k)$ is the dielectric constant given by Eq. (1). Performing the k integration we obtain

$$\phi(x) = -i \frac{\sigma_0 x_0}{\epsilon_0} \int_{-\infty}^{\infty} \frac{e^{ikx}}{kK(\omega, k)} \frac{dk}{2\pi}. \quad (7)$$

The integration is to be taken along the real k axis as

⁵ The excitation of electron waves has been treated by W. E. Drummond [Rev. Sci. Instr. 34, 779 (1963)] and by M. Feix, Ref. 7.

⁴ B. D. Fried and S. D. Conte, *The Plasma Dispersion Function* (Academic Press Inc., New York, 1961).

shown in Fig. 1(A). The integrand has a pole at the origin which leads to a constant potential, different on the two sides of the grids. Since it does not contribute to the electric field we may ignore it.

We are at liberty to deform the contour of the k integration into the complex k plane. For positive x , which is all we consider since the potential is anti-symmetric in x ; it is convenient to deform part of the contour into the *upper* half-plane. First we note that (2) and (4) are valid only when the imaginary part of ω/kv is positive, i.e., when k is positive since ω_0 is assumed to have a very small positive imaginary part. For negative k a different expression is required, namely k must be replaced by $-k$ in expressions (2) and (4) since the dielectric constant is an even function of the wave number k . For this reason we split the integral in (7) into two parts:

$$\phi(x) = -i \frac{\sigma_0 x_0}{2\pi \epsilon_0} \left[\int_{-\infty}^0 \frac{e^{ikx} dk}{kK(\omega_0, -k)} + \int_0^{\infty} \frac{e^{ikx} dk}{kK(\omega_0, k)} \right], \quad (8)$$

and treat each part separately.

The first integral in (8) involves the use of the derivative of the plasma dispersion function $Z'(\zeta)$ in the *upper* half plane where it was originally defined. The first integrand is, therefore, free from singularities except for a simple pole at⁵

$$k \approx i \left[2 \left(\frac{\omega_{pe}}{v_e} \right)^2 + 2 \left(\frac{\omega_{pi}}{v_i} \right)^2 \right]^{1/2} = ik_D \quad (9)$$

which will give an exponential contribution. It is convenient to deform the contour of the first integral so that it runs *in* along the *positive* real k axis as shown in Fig. 1(B). Now the real and imaginary parts of $Z'(\zeta)$ are even and odd functions of the (real) argument ζ so we can write

$$\phi(x) = \frac{\sigma_0 x_0}{\epsilon_0} \left[\frac{e^{-k_D x}}{2} + \frac{1}{\pi} \int_0^{\infty} \frac{1}{k} \operatorname{Im} \left\{ \frac{1}{K(\omega_0, k)} \right\} e^{ikx} dk \right], \quad (10)$$

where $\operatorname{Im}\{ \}$ stands for the imaginary part of the quantity in braces. We shall only be concerned with the integral contribution, since the exponential is significant only within a few Debye lengths from the source. Introducing dimensionless variables appropriate to ion-acoustic waves

$$\Phi = -\epsilon_0 \phi / \sigma_0 x_0; \quad \omega_0 x / v_i = z; \quad \omega_0 / \omega_{pi} = f; \\ kv_i / \omega_0 = \eta; \quad T_i / T_e = T; \quad v_i / v_e = V,$$

we obtain for the integral contribution to Φ

$$\Phi = \frac{f^2}{\pi} \int_0^{\infty} \operatorname{Im} \left\{ \frac{-\eta}{\eta^2 f^2 - Z'(1/\eta) - TZ'(V/\eta)} \right\} e^{i\eta z} d\eta. \quad (11)$$

This is a one-sided Fourier transform, or a LaPlace transform. Considerable insight into the behavior of $\Phi(z)$ can be gained by considering the integrand for various limiting arguments (always for $f^2 \ll 1$):

I. $\eta \ll V, \quad Z'(V/\eta) \approx \eta^2/V^2, \quad Z'(1/\eta) \approx \eta^2,$
 $\operatorname{Im}\{ \} \approx 0; \quad (12a)$

II. $V \ll \eta \ll 1, \quad Z'(V/\eta) \approx -2 - 2\pi^{1/2}i(V/\eta), \quad Z'(1/\eta) \approx \eta^2,$
 $\operatorname{Im}\{ \} \approx \frac{V}{T} \frac{\pi^{1/2}}{2}; \quad (12b)$

III. $1 \ll \eta \ll 1/f, \quad Z'(V/\eta) \approx -2, \quad Z'(1/\eta) \approx -2 - 2\pi^{1/2}i \frac{1}{\eta},$
 $\operatorname{Im}\{ \} \approx \pi^{1/2}/2(1+T)^2; \quad (12c)$

IV. $1/f \ll \eta < \infty, \quad Z'(V/\eta) \approx -2, \quad Z'(1/\eta) = -2,$
 $\operatorname{Im}\{ \} \approx 0. \quad (12d)$

We see that the transform function, which is always real, takes on different, approximately constant values for different arguments, with jumps occurring at the rather widely separated points $\eta \approx 0.6V, 0.6, 1/f$. This result is summarized in Fig. 2.

Integration of Eq. (11) once by parts shows that $\Phi(z)$ is equal to $-1/iz$ times the transform of the *derivative* of $\operatorname{Im}\{ \}$ (the derivative is also shown in Fig. 2).

Since the jumps are well separated Φ may be seen to consist of three distinct parts, each arising from one of the jumps and each with a different characteristic length. If the jumps were actually discontinuous at $\eta = \eta_0$ then the contribution would be of the form $(-1/iz)$ times an undamped exponential $e^{i\eta_0 z}$. Since each jump has a width there is further damping with a damping length inversely proportional to the half-width

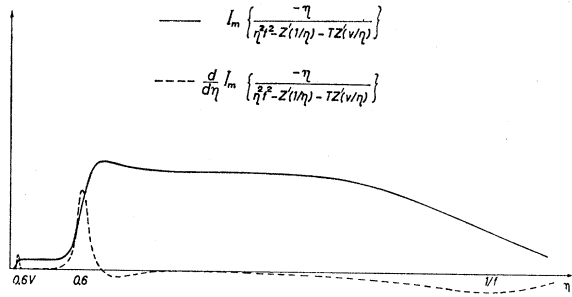


FIG. 2. Behavior of the transform function and its derivative along the real k axis.

of the jump. We now consider each contribution in more detail.

We first note that, for our purposes, the contributions from the jump at $\eta \approx 1/f$ has a characteristic length equal to the Debye length and is important only very near the source. As is easily seen, the other two contributions are proportional to $1/z$ for small z and the fact that the transform falls to zero in the vicinity of $\eta \approx 1/f$ simply means that for distances closer than a few Debye lengths the potential no longer increases as $1/z$. In fact it approaches a constant given by the total area under the transform curve

$$\Phi(0) \approx \frac{\pi^{1/2} f}{2(1+T)^{3/2}} \quad f \ll 1. \quad (13)$$

We do not consider the form of this contribution any further.

We next consider the contribution from the "jump" in the vicinity of $\eta \sim 0.6$. In this region, the approximate dielectric constant (4) applies, i.e., the electrons behave essentially as massless particles which equilibrate instantaneously with the fluctuating potential [$Z'(\omega/kv_e) \approx -2$] and the vacuum-displacement current is negligible compared with the electron and ion currents. With the aid of Ref. 4 we find that the jump occurs at $k \approx 0.62(\omega_0/v_i)$ and the derivative has a width (at half-maximum) of about $\Delta k = 0.24(\omega_0/v_i)$. Thus we expect a damped wave $\Phi \sim (e^{-0.24z/z})e^{-i0.62z}$. This result is not very accurate, however, since the derivative curve does not have a Lorentzian shape. We have, therefore, evaluated (11) numerically, using the IBM 7090 computer, to obtain the precise behavior of the potential.⁶ Since the quantity Φ/f^2 is independent of frequency provided $f^2 \ll 1$, it is this quantity which we shall discuss. Figure 3 shows the magnitude (semilog plot) and phase of Φ/f^2 . The curve marked $m_e/m_i = 0$, which corresponds to the approximation $Z'(\omega/kv_e) = -2$, will be discussed first.

For $z \ll 1$ the exact location and shape of the jump are unimportant and after integration of (11) by parts

⁶ A brief discussion of the method of evaluation and of errors is given in the Appendix.

once one obtains

$$\frac{\Phi}{f^2} = -\frac{1}{\pi} \frac{1}{-iz} \frac{\pi^{1/2}}{2(1+T)^2}, \quad \frac{1}{f} \ll z \ll 1. \quad (14)$$

For $z \gg 1$ and $m_e/m_i = 0$ the behavior is very nearly exponential. To a good approximation the behavior in this region can be represented by a single complex wave vector:

$$k = (0.590 + i0.243)\omega_0/v_i \quad (15)$$

which indeed corresponds closely with the first entry in Table I.

For realistic values of m_e/m_i , Fig. 3 shows that the decay of the ion wave is eventually limited by the contribution from the jump near $kv_i/\omega_0 = 0.6V$ which is associated with electrons. This contribution is much smaller in magnitude [by a factor of roughly 4V as may be seen by comparing (12b) and (12c)] but has a much greater characteristic length ($\Delta k \sim \omega_0/v_e$) and hence may be expected to dominate at large distances. Furthermore, there is an interference between the two contributions in the region where they have comparable

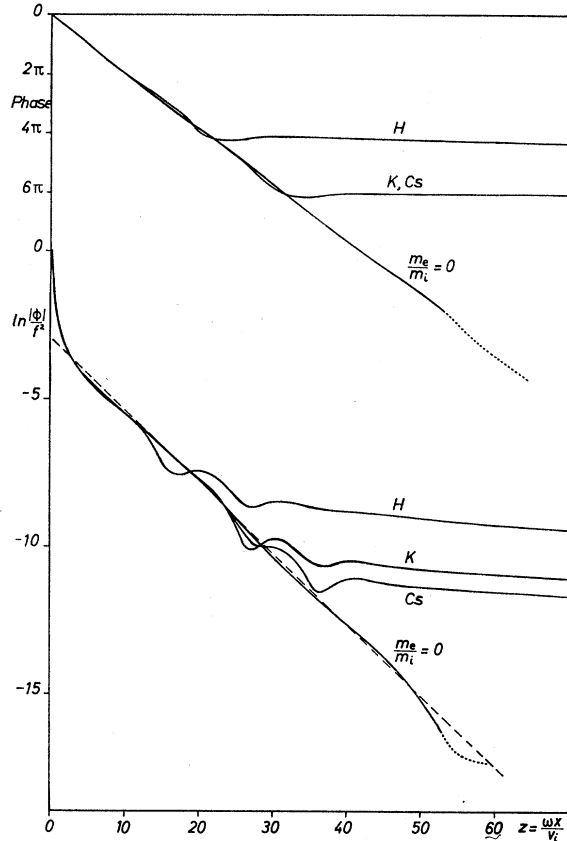


FIG. 3. Magnitude (semilog plot) and phase (linear plot) of the potential due to a pair of grids in plasmas with different ion species (hydrogen, potassium, cesium, and the limiting case $m_e/m_i = 0$), $\omega_0 \ll \omega_{pi}$. Dashed line shows single pole approximation of Sec. IV.

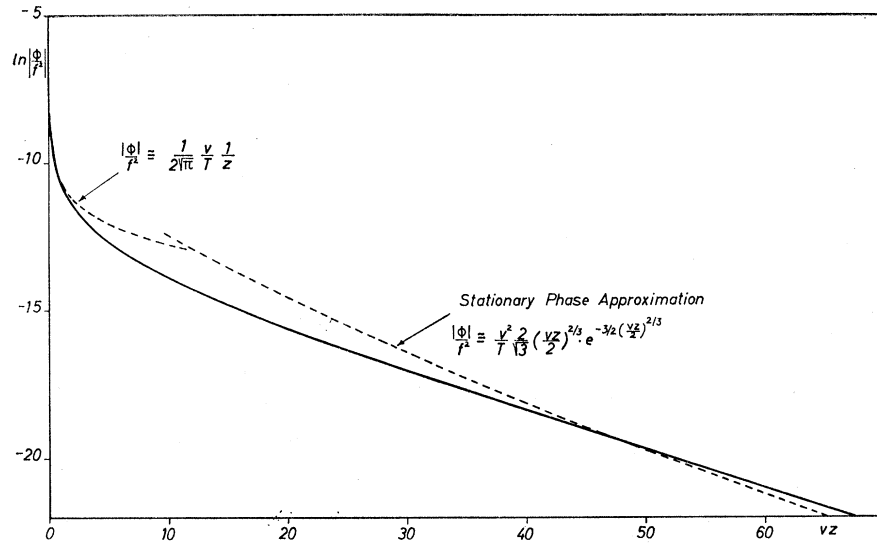


FIG. 4. Magnitude (semilog plot) of the electron contribution to the potential, which dominates far from the source.

amplitudes. The period of the interference pattern is governed by the ion wave contribution since it has the shortest wavelength.

We now examine the electron contribution in more detail. We may let $Z'(1/\eta) \approx \eta^2 \ll 1$ and write $\xi = \eta/V$, obtaining

$$\Phi/f^2 \approx \frac{V^2}{T} \frac{1}{\pi} \int_0^\infty \text{Im} \left\{ \frac{\xi}{Z'(1/\xi)} \right\} e^{i\xi(Vz)} d\xi, \quad (16)$$

thus making evident the change in length scale and the smaller magnitude of this contribution. This contribution has also been evaluated numerically and is shown in Fig. 4. For small z , only the magnitude of the jump (not its precise shape) is important and

$$\Phi/f^2 \approx \frac{1}{2\pi^{1/2}} \frac{V^2}{T} \frac{1}{-iVz}, \quad Vz \ll 1. \quad (17)$$

Furthermore, the jump occurs at $k = 0.6\omega_0/v_e$ and its derivative has a width $\Delta k \approx 0.2\omega_0/v_e$. This introduces an additional damping and phase shift on a distance scale which corresponds to propagation at the electron thermal speed. For very large Vz , we can use the small-argument approximation,⁴

$$Z'(1/\xi) \approx \xi^2 + 2\pi^{1/2}i(1/\xi)e^{-(1/\xi^2)},$$

in Eq. (16) and the method of stationary phase to evaluate the resulting integral. We obtain:

$$\Phi/f^2 = (V^2/T) (2/\sqrt{3}) (\frac{1}{2} Vz)^{2/3} e^{i2\pi/3} \times \exp[\frac{3}{2} (\frac{1}{2} Vz)^{2/3} (\sqrt{3}i - 1)], \quad Vz \gg 1. \quad (18)$$

This result has already been obtained by Feix⁷ in the study of the excitation of electron oscillations by grids when $\omega_0^2 \ll \omega_{pe}^2$. Note that $f^2 V^2/T = \omega_0^2/\omega_{pe}^2$ and $Vz = \omega_0 x/v_e$ so the ion variables disappear entirely. A

similar result was obtained by Landau² for the half-space problem.

We have seen that Φ/f^2 depends on the frequency only through the dimensionless distance variable $z = \omega_0 x/v_e$ so long as the frequency is small compared with the ion plasma frequency ($f^2 \ll 1$). When the frequency is increased above the ion plasma frequency,

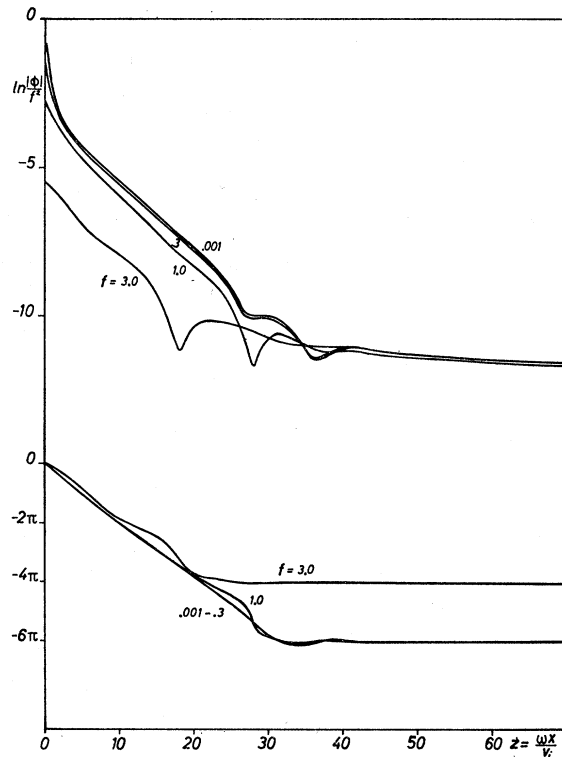


FIG. 5. Effect of increased driving frequency on the potential (Φ/f^2), cesium plasma with $T_e = T_i$.

⁷ M. Feix, Phys. Letters 9, 123 (1964).

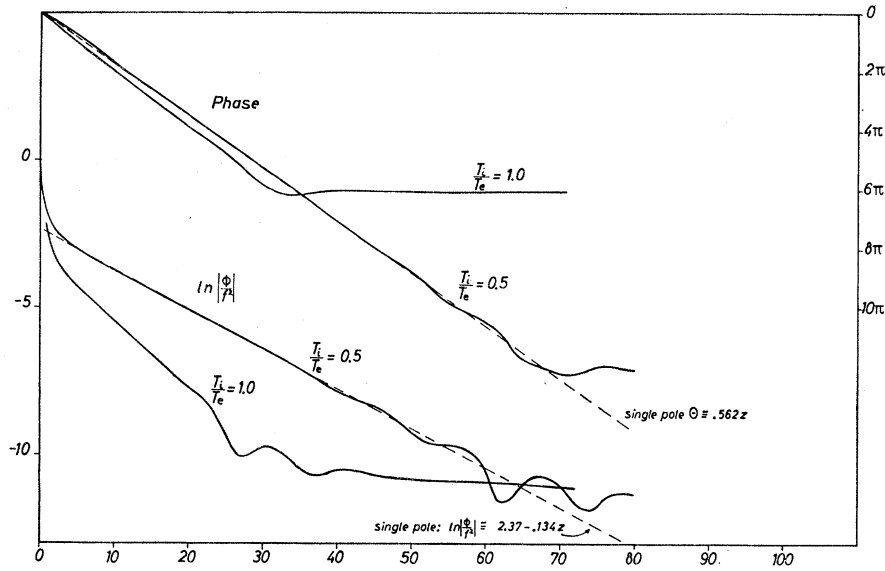


FIG. 6. Effect of decreasing T_i/T_e in a cesium plasma. Dashed curve shows single pole approximation for $T_i/T_e=0.5$.

the jump at $\eta=1/f$ coalesces with the jump at $\eta \approx 0.6$ and annihilates it, thus reducing the ion wave excitation coefficient. In Fig. 5 we show the behavior of a cesium plasma as the frequency is increased above the ion-plasma frequency. It is seen that the ion wave may be excited at the ion-plasma frequency and slightly above with reduced amplitude. As a practical matter, however, the wavelength of such a wave is comparable with Debye length and the contribution from the pole [Eq. (9)] can probably no longer be neglected.

It has previously been shown³ that the consequence of an electron temperature greater than the ion temperature is to reduce the damping of ion waves. This has the effect of increasing the distance over which the ion wave follows an exponential decay although the number of e -folding distances until the electron contribution becomes dominant is nearly the same. Figure 6 shows the behavior for $T_i/T_e=0.5$ and 1.0 in a cesium plasma.

IV. CONCLUDING REMARKS

We have shown, by numerical computation, that there is a region neither too near, nor too far, from the source in which an exponentially damped ion wave exists. It is of interest to try to explore other possible integration contours which will lead directly to this result. Such a contour is shown in Fig. 1(C). We have again brought the incoming and outgoing contour together in the upper half-plane and in doing so have passed over the pole at $k \approx ik_D$ (which we neglect) and the first three of the poles listed in Table I (located at $\eta = \eta_j$). Using approximation (2) and evaluating the residues,

$$\Phi/f^2 = i \sum_{j=1}^J \frac{\eta_j^3}{Z''(1/\eta_j)} e^{i\eta_j z} + \chi(z), \tag{19}$$

where $\chi(z)$ is the contribution from the contour C' . The pole contributions are readily evaluated using Ref. 4. For $T_e = T_i$ and $\omega_0 \ll \omega_{pi}$

$$\Phi/f^2 = i \{ \exp[(-2.92 - 1.18i) + (-0.243 + 0.59i)z] + \exp[(-5.8 - 0.38i) + (-0.204 + 0.259i)z] + \dots \} + \chi(z). \tag{20}$$

It may be seen that near the source the contribution from the first pole is larger than the contributions from the next few poles, even though the latter decay more slowly with distance, because of the larger coefficient. It is difficult to evaluate $\chi(z)$. However, the numerical calculations indicate that the first term of Eq. (19), arising from the *most damped pole* and shown by a dashed line in Figs. 3 and 6, is a relatively good approximation over a limited but nevertheless useful region.

Although these results have been obtained for a pair of grids with arbitrarily close spacing ($x_0 \rightarrow 0$), they are easily generalized to finite x_0 since we have effectively obtained the Green's function for the problem. Thus we see that so long as $x_0 \ll v_i/\omega_0$, i.e., small compared to the wavelength of the ion waves, the results are still valid. Since the surface charge density is related to current density I_0 supplied to the grids through the relation $I_0 = -i\omega_0\sigma_0$,

$$\frac{\sigma_0 x_0}{\epsilon_0} = \frac{I_0 x_0}{-i\omega_0 \sigma_0} = \frac{I_0}{-i\omega_0 C}, \tag{21}$$

where C is the capacitance per unit area of the grids without plasma. Thus, for a constant current source σ_0 varies inversely with frequency and the ion wave excitation increases only linearly with frequency. The sensitivity of a second pair of grids, which responds to the electric field, will also be proportional to frequency when connected to a high-impedance load.

Since the experiment by Wong *et al.*¹ has demonstrated the feasibility of detecting ion waves it may also be possible, by extending the sensitivity of the receiver, to observe the electron contribution at larger distances. The use of a higher frequency would have the twofold benefit of increasing the excitation coefficient and decreasing the distance required between the transmitting and receiving grids. Furthermore, departures from exponential damping should be readily detectable near the source.

ACKNOWLEDGMENTS

It is a pleasure to acknowledge several stimulating conversations with B. D. Fried and with M. Feix concerning this problem. This work has been undertaken as part of the joint research program of the Institut für Plasmaphysik and EURATOM. This work was done while the author held a National Science Fellowship for research at the Institut für Plasmaphysik.

APPENDIX: NUMERICAL EVALUATION AND THE TRANSFORM INTEGRAL

Since the quantitative aspect of the results given in Figs. 3-6 depend upon the numerical evaluation of the transform integral, Eq. (11), we have a short discussion of the method employed and of possible errors. The integral (11) was first replaced by a sum

$$\frac{\Phi^*}{f^2} = \frac{\Delta\eta}{\pi} \sum_{m=1}^M F(m\Delta\eta) e^{im\Delta\eta z}, \tag{A1}$$

where $F(\eta)$ denotes the transform function. We observe that the substitution of an *infinite* sum ($M = \infty$) for the integral is equivalent to multiplication of the transform function by a "comb" function, with periodicity $\Delta\eta$, in (11). Thus (A1) defines a new function which is just the convolution of the original function with the periodic function,

$$P(z) = \sum_{l=-\infty}^{\infty} \delta(z - 2\pi l / \Delta\eta),$$

i.e.,

$$\Phi^*(z) = \sum_{l=-\infty}^{\infty} \Phi(z - 2\pi l / \Delta\eta). \tag{A2}$$

Thus, in order that (A1) be a good approximation to the original function, we must select $\Delta\eta$ such that

$$\Delta\eta < \pi / z_{\max},$$

where z_{\max} is the largest value of z to be used. The function $\Phi(z)$ must decrease sufficiently rapidly outside this range.

Truncation of the sum (A1) after a finite number of terms is equivalent to introducing another jump in the transform (11) and according to the argument of Sec. III this introduces an extraneous term which decays slowly with z , although it oscillates rapidly [$\Phi \sim (A/iz)e^{iM\Delta\eta z}$, $A = F(M\Delta\eta)$]. This difficulty was effectively eliminated through the use of a Gaussian cutoff, i.e., through the substitution of $e^{-\frac{1}{2}(\eta/\eta_0)^2} F(\eta)$ for $F(\eta)$ in (A1). To be sure, a discontinuity is still introduced at $\eta \approx M\Delta\eta$, but η_0 can be selected so as to make the magnitude of the jump negligibly small by requiring

$$\eta_0 > M\Delta\eta/6. \tag{A3}$$

Multiplication of the transform function by the Gaussian function is equivalent to the convolution of the original function with another Gaussian function of z , i.e., it represents a *smoothing* operation with a scale $\Delta z \cong 1/\eta_0$. The results presented in Figs. 3-6 have been smoothed ($\Delta z \cong 0.2$) due to this effect. This is believed to be of little or no consequence except very near to the origin.

Finally, machine round-off errors become important in the region far from the source where there is a high degree of cancellation between the individual terms of (A1). Each term is of order unity, and assuming individual random errors of the order $10^{-8.4}$ we estimate an error of

$$\epsilon \approx (1000)^{1/2} \times 10^{-8.4} \approx e^{-16} \quad (\text{for } M = 1000) \tag{A4}$$

which is very much smaller than the quantity computed except for the nonphysical case $m_e/m_i = 0$ (see Fig. 3). Here Φ/f^2 was observed to decay to roughly this value at $z \cong 50$ and to be masked by irregular fluctuations of the above magnitude beyond this point. Uncertainties in the region $53 < z < 60$ are indicated by the dotted portion of the curve in Fig. 3.

Systematic errors larger than the above by an order of magnitude probably also arise in the computation of the complex exponential and the plasma dispersion function used in evaluating the individual terms of (A1). It is difficult to estimate the size of these errors but it has been shown [by comparison with the result computed using Eq. (16)] that they do not significantly affect the results in the region where the weak and slowly decaying electron contribution prevails ($z > 30$ in Fig. 3).